SAND2011-6511C

Carbon MEMS Accelerometer

Jennifer Strong*[1], Cody M. Washburn[2], Randy Williams[3], John McBrayer[3], Tedd Rohwer[3], Regan Stinnett[3], Patrick Finnegan[1], Brad Hance[2], Doug Greth[4], and Dave R. Wheeler[5]
[1]LMATA Government Services, LLC, Albuquerque, NM 87109
[2] Organic Materials Department Sandia National Laboratories
[3] Advance Electronics and Devices Department Sandia National Laboratories
[4] Micro-Fabrication Department Sandia National Laboratories
[5] Department of Bio and Nano-material development Sandia National Laboratories
*Corresponding author: Sandia National Laboratories, Albuquerque, NM 87185, jmstron@sandia.gov

Abstract: The newly emerging field of carbon-based MEMS (C-MEMS) attempts to utilize the diverse properties of carbon to push the performance of MEMS devices beyond what is currently achievable. Our design employs a carbon-carbon composite using nano-materials to build a new class of MEMS accelerometer that is hyper-sensitive over a dynamic range from micro-G to hundreds of G's – far surpassing the capabilities of currently available commercial MEMS accelerometers.
Validating single cantilever beams of a 10:1 aspect ratio has shown only a 2% error from predicted to actual deflected calculations,while a clamped-clamped U-beam with 5% carbon nanotubes described nearly a 30% increase in Young's modulus and begins demonstrating tunable material properties through nano-material loading in MEMS devices.

Keywords: carbon MEMS, C-MEMS, carbon-carbon composites, accelerometer

1. Introduction

A carbon-carbon composite MEMS accelerometer, using nano-material stiffeners, drives new materials and devices into micro-electro mechanical systems to improve dynamic range, sensitivity, lifetime, and functionality when compared to state of the art MEMS technology. The proposed carbon composite structure is a replacement for single crystal/metal MEMS beams, flexures, struts etc. at a fraction of the expense. These materials are less prone to stiction under high G-force loading, and have tremendous resilience under extreme mechanical deformation and shock.
The pyrolysis of photo-patternable materials has been described by George Whitesides, et. al. [1], which describes the basic micro-electromechanical properties related to pyrolytic carbon materials and resonator devices. Since, Marc J. Madou, et. al.[2] U.C. Irvine and Richard L. Mcreery, et. al.[3] University of Alberta, CA developed carbon on carbon approaches to develop carbon micro-electromechanical systems, high surface area electrochemical sensors, along with carbon for anode/cathode materials for Li-ion battery applications. Groups at Sandia have demonstrated pyrolyzed carbon's remarkable abilities by electrochemically placing nano-materials on the surface for bio-applications [4].

The MEMS single beam, clamped-clamped U-beam and diaphragm carbon-carbon composite structures provide the basis of testing and evaluating nano-materials in patterned carbon matrices. Nano-material loading into various polymer precursors and carbon matrices has been shown [5,6] to directly impact spring constant and Young's modulus of the final material. Modeling and validating nano-material structures is a new challenge to finite elemental analysis (FEA) and this is an initial attempt to start merging data collected with modeling efforts.

2. Device Fabrication

Devices are fabricated using a 4 inch silicon 1-100 ohm-cm wafer, which are cleaned using acetone, methanol and isopropanol and dried with N2. Hexamethyldisilazane (HMDS), an adhesion promoter and dehydration bake prime the wafers for photolithography in an HMDS oven. The vapor primed wafers are spin coated to a thickness of 3.3 μm with photoresist Clariant Chemical - AZ4330. Using a manual contact aligner, Karl Suss MA6, the wafers are exposed to 120 mJ/cm^2 of 365 nm light. The exposed resist is then developed using MF319 for approximately 125 seconds. A modified post exposure bake process is used by ramping a hotplate from 90 C, 10 C/min ramp, and holding at an elevated temperature of 280 C for 1 minute.

Pyrolysis to carbon is done under a high temperature reducing atmosphere producing a mechanical structure which is electrically active. A 3 C/ min. ramp rate is used with a Lindberg 3"

tube furnace and a CoorsTek alumina tube of 5% hydrogen and 95% nitrogen atmosphere. The program holds at 1100 C for 1 hour before passively cooling to room temperature. At this point the devices are released from the silicon substrate by using a xeon difluoride etch process of 65 cycles to undercut the silicon away from the carbon by 85-90 μm.

Single cantilever beams, clamped-clamped U-beams and a diaphragm with a large proof mass were designed and fabricated using this approach, shown in Figure 1(a-c).

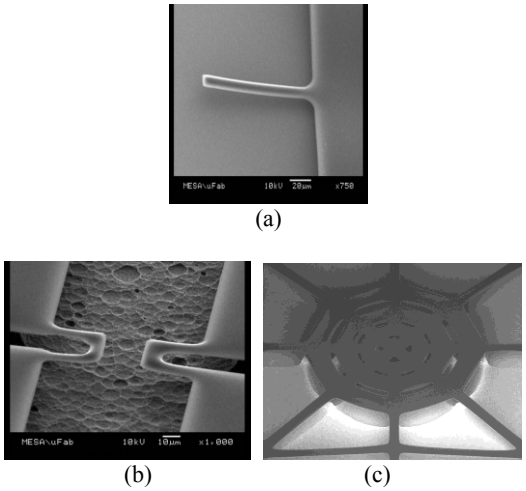

(a) (b) (c)

Figure 1. The (a) single cantilever beam, (b) clamped-clamped U-beam, and (c) proof mass diaphragm carbon MEMS device.

2.1 Multiwalled Carbon Nanotube Blending

Multiwalled carbon nantubes (MWCNT) were purchased from Nanostructured and Amorphous Materials Inc., with a distribution of 40-70 nm in diameter and 0.5 μm to 5.0 μm in length and blended in at 1%, 5%, 7% and 10% weight percent to Clariant chemical AZ4330 photoresist. The same resist process was used, which included a 2 hour sonication step before spin coating to help minimize agglomeration of the nanotubes. Pyrolysis is necessary before etching as to allow the stress of the material to be conformal with the starting silicon substrate. The same xeon difluoride etch parameters were used to develop the clamped-clamped U-beam design, which is shown in Figure 2(a-d).

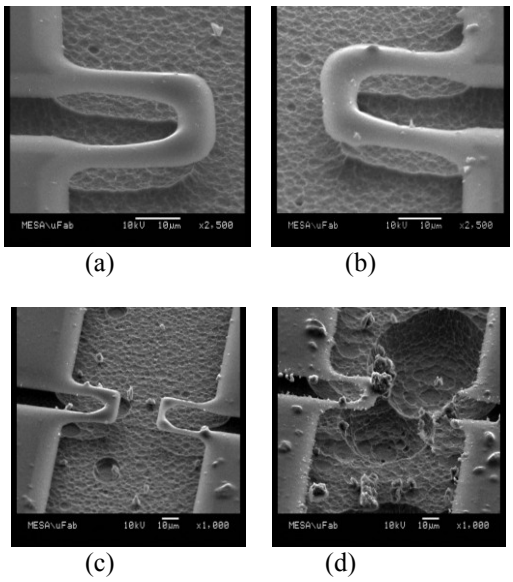

(a) (b) (c) (d)

Figure 2. SEMS of (a) 1%, (b) 5 %, (d) 7%, and (e) 10% clamped-clamped U-beam designs after etch release.

2.2 Device Dimensions and AFM Testing

During processing of the devices, the photo-active polymer passes through the glass transition temperature (Tg) approximately at 180 C before hardening to Bakelite. At this stage the lithographic mask dimensions and the final carbon device dimensions are biased due to the reflow of the photoresist. Table 1 describes the device investigated and the final geometry of the unloaded (no tubes) carbon MEMS device tested under AFM.

Table 1. Lithographic Definitions.

	Mask		Device		
Device	L (μm)	W (μm)	L (μm)	W (μm)	Thickness (μm)
Single Beam	100	10	106	11.6	1.0
U-Beam(w)	30	10	27	8.5	0.8
U-Beam(s)	30	7.5	27	6.0	0.8

The proof mass diaphragm device will be discussed as a separate section due to the complex geometries involved.

A Veeco D500 atomic force micrscopy (AFM) tool was used to evaluate the devices in terms of force verse deflection measurements. Aluminum contact mode tips were purchased from Budget Sensors, model number: ContAl-G-10, with a resonant frequency of 13KHz (+/- 4KHz) and force constant of 0.2 N/m with a range of 0.07 to 0.4 N/m. Force verse distance data was collected using 1 V bias or 50 nano-Newtons (nN) of down force, and a scan rate of 3.49 Hz using a 0.329 N/m tip. The above software and hardware configuration was used for all data collected.

3. COMSOL Multiphysics and Beam Theory

The use of COMSOL Multiphysics begins with a simple correlation of COMSOL geometry models to physical data. The purpose is two-fold: first, it allows a control on experiments by properly extracting material properties from our test structure data. Second, it helps to ensure that modeling complex design geometries in COMSOL yields practical and usable data and allows MEMS designers to build meaningful predictions.

Nano-material composites in MEMS fabrication have material properties that are either non-existent or poorly characterized in present literature. Investigating stationary structural mechanics and Young's modulus (E) in carbon-carbon composites in particular is an ongoing effort to understand the fundamentals. Therefore, COMSOL guides approximations to ensure that raw data collected and distillation of Young's modulus from physical test structures is reasonable. After calculating Young's modulus from test structure data using beam theory, that value of E into the COMSOL model of that structure to make certain that the modeled deflection in COMSOL is reasonably close to the deflection expected from AFM force versus deflection curves.

Next, correlating test data for more complex geometries to their corresponding COMSOL models. Good correlation gives confidence that accurately modeled physical structure in COMSOL can be used for design applications. A poor correlation yields information as well, pointing to either a disparity between our COMSOL model and design, or a misunderstanding between structures due to fabrication error which are coupled with complex nano-material interactions.

A successful correlation of complex geometries to corresponding models in COMSOL, will guide design optimization by enabling us to parametrically sweep through a wide range of key dimensions for each design and fine-tune the design for the desired responses. Using COMSOL for the design optimization phase will considerably shorten both the time required and the materials consumed for optimization by freeing us of the necessity of fabricating and testing scores of structures with small design variations.

3.1 Cantilever Beam Theory

Cantilevered beams, and can be approximated by a linear beam of rectangular cross section with one fixed end and one free end. The force load (F) is applied to the free end of the beam. The beam has a given length (L), width (b), and thickness (h). Equation 1, gives the theoretical maximum deflection (δ) of such a beam, where E is Young's modulus and I is the second moment of inertia.

$$\delta = \frac{FL^3}{3EI} \qquad [1]$$

For a beam with a rectangular cross section, I can be calculated using Equation 2.

$$I_x = \frac{bh^3}{12} \qquad [2]$$

Using the expression for I given by Equation 2, Equation 1 can be re-written as Equation 3.

$$\delta = \frac{4FL^3}{bh^3E} \qquad [3]$$

In this case, the value of E is an unknown. From AFM data, basic measurements of beam deflection under a given force provide insight of mechanical movement. Approximating, the force versus deflection is linear for our measurement range, and follows the basic elastic relationship given by Equation 4, where k represents the theoretical spring constant of the cantilever beam in N/m.

$$k = \frac{F}{\delta} \quad [4]$$

After using Equation 4 to calculate an average theoretical spring constant (k) for a specific cantilever structure using our AFM data, Equation 5 determines the theoretical deflection (δ) of the beam for a given value of F.

$$\delta = \frac{F}{k} \quad [5]$$

Knowing the theoretical deflection (δ) for a given force (F), we re-arrange Equation 3:

$$E = \frac{4FL^3}{bh^3\delta} \quad [6]$$

Whick is followed by Equation 6 to calculate a value for Young's modulus (E).

3.2 U-Beam Calculations

Test structures included u-shaped beams which are clamped on both ends with the center of the beam free to deflect (see Figure 1(b)). When gathering force versus deflection data for these beams using the AFM, The AFM tip is centrally located with respect to thecenter of the free end of the beam and beam width.

When using these beams to calculate Young's modulus (E), we treat the u-beam as two single simple cantilevered beams with the applied force (F) evenly distributed between the two cantilevers. This allows us to compute E using Equation 6. The applied force for a single beam is assumed to be the force applied to the u-beam divided by 2.

COMSOL verified the validity of these assumptions. A comparison modeling of a u-beam made from aluminum, in COMSOL and was subjected to a point load on the free end of the beam along the beam's axis of symmetry, then looked at the corresponding maximum deflections of the beam for a range of load values A single cantilever beam version of the u-beam (essentially one side of the u-beam minus the bent portion of the beam), made from aluminum, was subjected to a point load on the free end with the maximum deflections of the beam captured. For any given load applied to the u-beam, the maximum deflection was 6.21% more than that of the cantilever (with the loading applied to the cantilever divided by two to approximate the full load being distributed over 2 cantilevers).

3.3 Modeled Beams

All of the COMSOL models start with the mask dimensions and are adjusted t to account for various differences between the dimensions on the mask and final product. These differences are mentioned briefly in Section 2.2. Specifically the final length and width dimensions are adjusted slightly, some rounds are added to some of the corners to approximate the reflow of photoresist, and an undercut is added at the edge of the bond pads to approximate the lateral material removal that happens during the etch process. These adjustments can vary from wafer to wafer as the fabrication process is still undergoing research and development. Examples of some specific COMSOL models used for the single cantilever beam structures and the u-beam structures are shown in Figure 3.

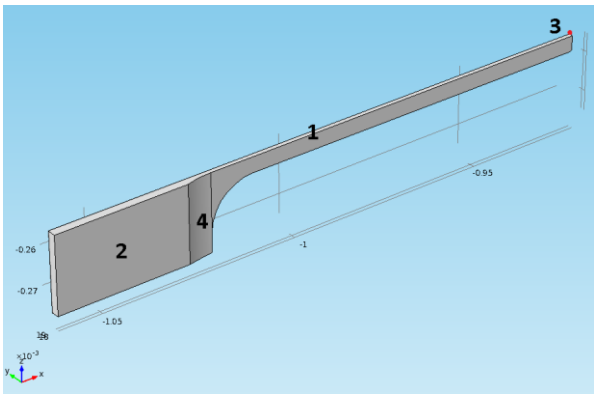

(a)

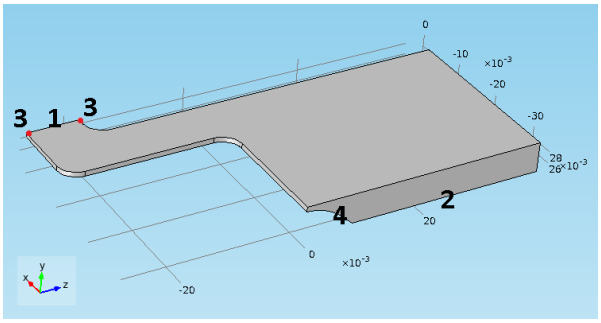

(b)

Figure 3. COMSOL models of the (a) single cantilever beam and (b) clamped-clamped u-beam.

For both models, "1" represents the location of a symmetry boundary, "2" is the bottom of the bond pad which is a fixed surface, "3" represents the location of the point loads (which are applied in the –y direction), and "4" is the undercut area due to the etch. For the u-beam, the point load is first applied to the far end of the beam and the deflection is measured; then, the point load is applied to the part of the "u" that is closer to the fixed end and the deflection is measured again. These two deflections are averaged to get the final modeled deflection.

3.4 Modeled Diaphragm Structure

The diaphragm structure, pictured in Figure 1(c), is one of the designs that we are most interested in at this time. This design is currently being looked at from a strictly mechanical perspective, but ideally the modeling will eventually encompass all of the electromechanical properties that are of importance to the functioning of the final device. The COMSOL model of the diaphragm structure is shown in Figure 4.

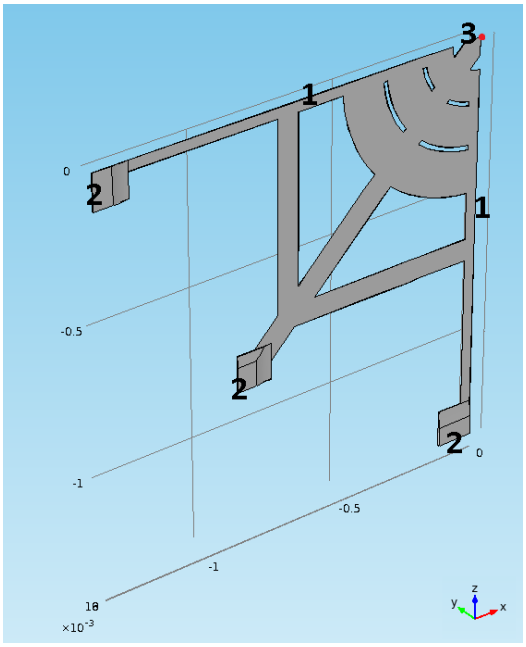

Figure 4. The COMSOL model of the diaphragm structure.

The labels "1," "2" and "3" hold the same meaning for Figure 4 as for Figure 3. The undercut area can be seen near the 3 fixed boundaries that represent the bond pads.

4. Data and Modeling Results

4.1 Single Cantilever Beam

Collection force versus deflection data for a set of 10 10μm cantilever beams made from 0% CNT loaded pyrolytic carbon, averaged the theoretical spring constant for all 10 beams, and then extracted a value for Young's modulus (E). The value obtained for E from this particular wafer was larger compared to values of E that obtained from the u-beam structures (5.236E+10 versus 2.227E+09 Pa). Standardization of the fabrication process for a particular geometry of interest and more data will hone the average theoretical spring constant for the test structures. COMSOL modeling did an excellent job of predicting the deflection for this particular cantilever structure. The predicted deflection was 4.03E-07 m for an applied force of 50nN, and the modeled deflection was 4.11E-07 m, a difference of ~2%.

4.1 U-Beam carbon-carbon composite

AFM data of u-beam structures loaded with MWCNTs at varying weight percent was attempted to be correlated. Collection of force versus deflection (δ) data for 4 u-beams, 2 wide u-beams and 2 skinny u-beams, for each composite were investigated. Use of this data enabled calculation of an average Young's modulus (E) for each composite. Table 2 shows the calculated values of E for each composite.

Table 2. Young's Modulus vs. CNT Loading.

CNT Loading	Young's Modulus (Pa)
0%	2.227E+09
1%	2.165E+09
5%	3.061E+09
7%	1.944E+09
10%	2.161E+09

The structures made from the 7 and 10% CNT loaded composites had fabrication issues due to the high loading of CNTs, as evidenced by the SEM images in Figure 2. This led to deflection measurements that are greater than expected, and consequently calculations for E that are likely

inaccurate as compared to the calculations for the 0, 1, and 5% CNT loaded composites.

Fabrication issues aside, the COMSOL u-beam models predicted deflection with low error for a given structure and a given value of *E* with a chosen point load of 50nN. The percent difference between the modeled deflection and the deflection derived from the theoretical spring constant extracted from the AFM data is small, as shown in Table 3 below.

Table 3. Modeled Versus Predicted Deflections for the U-Beam Structures.

Beam Type	% CNT Load	Modeled δ (m)	Predicted δ (m)	% Difference
wide	0%	1.93E-07	2.03E-07	4.97%
wide	1%	1.99E-07	2.09E-07	4.97%
wide	5%	1.41E-07	1.48E-07	4.92%
wide	7%	2.22E-07	2.33E-07	4.80%
wide	10%	2.00E-07	2.09E-07	4.68%
skinny	0%	2.90E-07	2.88E-07	0.79%
skinny	1%	2.98E-07	2.96E-07	0.71%
skinny	5%	2.11E-07	2.09E-07	0.56%
skinny	7%	3.32E-07	3.30E-07	0.72%

4.3 Diaphragm Structure

While collecting force versus deflection data for the 10μm cantilever beams, we also collected data for a set of 8 diaphragm structures off of the same wafer of 0% CNT loaded pyrolytic carbon structures. The averaged theoretical spring constant for all 8 structures was used to predict the deflection that we expected to see in the COMSOL model.

The diaphragm structure has a predicted deflection of 2.38E-07 m for an applied force of 50nN. This does not correlate well to the modeled result of 8.49E-07 m. We are still investigating the reason for the poor correlation. The diaphragm structures on this particular wafer appeared to have a significant amount of internal stress. See Figure 5 below.

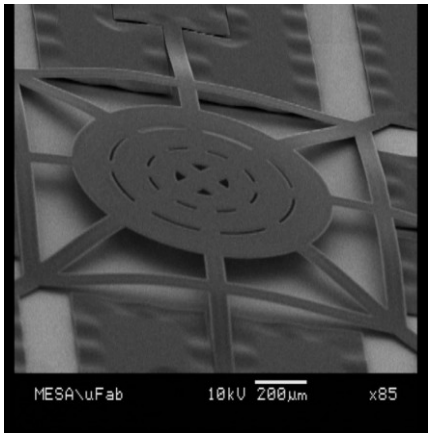

Figure 5. A recently fabricated diaphragm structure.

As illustrated in Figure 5, the diaphragm structure is bowed significantly out of plane. This could be affecting the force versus deflection measurements taken using the AFM, causing a poor correlation to the COMSOL model which is modeled as a flat, in-plane structure.

5. Conclusions

The development of a tunable material set using carbon nanotubes in an accelerometer has been demonstrated and investigated using COMSOL modeling to show a nearly 30% improvement in Young's modulus over pyrolytic carbon. The procedure to correlate and validate a finite element model is still being researched and developed, with as low as 2% error from single cantilever beams with a 10:1 aspect ratio. Device processing, polymer reflow, and carbon nanotube blending and suspension have critical components which relate to the final geometries of carbon MEMS devices and more data is required to optimize many of these hurdles.

A diaphragm designed accelerometer with a central proof mass has multiple complex geometries and pushes mechanical understanding and modeling of these carbon-carbon composite structures and devices. COMSOL will be essential in shortening and optimizing the design and manufacturing feedback schedule for future device fabrication.

6. References

1. G.Whitesides, et. al. “Fabrication and Characterization of Glassy Carbon MEMS”, Chem. Mat. 1997, 9, 1399-1406
2. M. Madou, et. al. “Fabrication of suspended carbon microstructures by e-beam writer and pyrolysis”,2006, (13), 2602-2607
3. R. Mcreery, et. al. ” Photoresist-Derived Carbon for Microelectomechanical Systems and Electrochemical application” Journal of The Electrochemical Society, 147, (1) 277-282
4. Polsky, et. al.” Lithographically Defined Porous Carbon Electrodes”, vol. 5, (24), 2792-2796
5. T. Yamada, et. al.” A stretchable carbon nanotube strain sensor for human motion detection”, Nature NanoTech., 3/27/2011, DOI: 10.1038
6. T. Ramanathan, et. al. “Functionalized graphene sheets for polymer nanocomposites”, Nature NanoTech., 6/2008, vol.3, DOI: 10.1038

7. Acknowledgements

The authors would like to thank Dick Grant, Christine Ford, Jeff Stevens, NINE funding, and other sponsored support of this work. Sandia is a multi-program laboratory operated by Sandia Corporation, a Lockheed Martin Company, for the United States Department of Energy’s National Nuclear Security Administration under contract DE-AC04-94AL85000.